

# CASIMIR: A high resolution, far-IR/submm spectrometer for airborne astronomy

M. L. Edgar\*, M. Emprechtinger†, A. Karpov†, R. Lin‡, S. Lin‡, F. Maiwald‡, I. Mehdi‡,  
D. Miller†, S. J. E. Radford†, F. Rice†, J. Ward‡§ and J. Zmuidzinas†

\* California Institute of Technology,  
MS 301-17,  
Pasadena, CA, 91125  
U.S.A.

Email: mick@submm.caltech.edu

†California Institute of Technology

‡Jet Propulsion Laboratory  
Pasadena, CA 91109

§Currently at Raytheon Company,  
Fort Wayne, Indiana, USA

**Abstract**—CASIMIR, the Caltech Airborne Submillimeter Interstellar Medium Investigations Receiver, is a far-infrared and submillimeter heterodyne spectrometer, being developed for the Stratospheric Observatory For Infrared Astronomy, SOFIA. CASIMIR will use newly developed superconducting-insulating-superconducting (SIS) mixers. Combined with the 2.5 m mirror of SOFIA, these detectors will allow observations with high sensitivity to be made in the frequency range from 500 GHz up to 1.4 THz. Initially, at least 5 frequency bands in this range are planned, each with a 4-8 GHz IF passband. Up to 4 frequency bands will be available on each flight and bands may be swapped readily between flights. The local oscillators for all bands are synthesized and tuner-less, using solid state multipliers. CASIMIR also uses a novel, commercial, field-programmable gate array (FPGA) based, fast Fourier transform spectrometer, with extremely high resolution, 22000 (268 kHz at 6 GHz), yielding a system resolution  $> 10^6$ . CASIMIR is extremely well suited to observe the warm,  $\approx 100$ K, interstellar medium, particularly hydrides and water lines, in both galactic and extragalactic sources. We present an overview of the instrument, its capabilities and systems. We also describe recent progress in development of the local oscillators and present our first astronomical observations obtained with the new type of spectrometer.

## I. INTRODUCTION

CASIMIR[1], the Caltech Airborne Submillimeter Interstellar Medium Investigations Receiver, is a far-infrared (FIR) and submillimeter, very high-resolution, heterodyne spectrometer. It is being developed as a first generation, Principal Investigator class instrument for the Stratospheric Observatory For Infrared Astronomy, SOFIA [2]-[4]. Observations with CASIMIR on SOFIA are expected to begin in 2013 and the instrument should be available to guest investigators soon after. It is anticipated SOFIA will eventually achieve a flight rate of up to 160 flights per year, with a lifetime of 20 years.

Species	Transition	Frequency (GHz)	$E_{\text{lower}}$ (K)	Atmospheric 1 mm H <sub>2</sub> O	Transmission SOFIA
CH	$F_1 \rightarrow F_2; J = 3/2^- \rightarrow 1/2^+$	536.76	0.0	0 %	97 %
H <sub>2</sub> <sup>18</sup> O	$1_{10} \rightarrow 1_{01}$	547.68	34.2	0 %	81 %
NH <sub>3</sub>	$1_0 \rightarrow 0_0$	572.50	0.0	0 %	94 %
H <sub>2</sub> <sup>18</sup> O	$2_{11} \rightarrow 2_{02}$	745.32	100.6	0 %	82 %
NH	$N = 1 \rightarrow 0; J = 2 \rightarrow 1$	974.48	0.0	0 %	96 %
H <sub>3</sub> O <sup>+</sup>	$0_- \rightarrow 1_0^+$	984.66	7.5	0 %	65 %
NH <sup>+</sup>	$3/2^+ \rightarrow 1/2^-$	998.90	0.0	0 %	95 %
HF	$1 \rightarrow 0$	1232.48	0.0	0 %	30 %
H <sub>2</sub> D <sup>+</sup>	$1_{01} \rightarrow 0_{00}$	1370.09	0.0	0 %	94 %
N <sup>+</sup>	$^3P J = 1 \rightarrow 0$	1461.13	0.0	0 %	92 %
<sup>16</sup> OH	$^2\Pi_{1/2} J = 3/2^+ \rightarrow 1/2^-$	1837.82	181.9	0 %	94 %
C <sup>+</sup>	$^2P J = 3/2 \rightarrow 1/2$	1900.54	0.0	0 %	88 %
CH <sub>2</sub>	$1_{10} \rightarrow 1_{01}$	1917.66	22.4	0 %	99 %
CO	$1_8 \rightarrow 1_7$	1956.02	751.7	0 %	90 %

Fig. 1. Comparison of atmospheric transparency for a selection of significant astronomical lines between good conditions on Mauna Kea and within the stratosphere

Initially, CASIMIR will cover a frequency range from 500 GHz up to 1.4 THz. The frequency coverage may eventually be expanded up to 2 THz. It will be capable of covering this range at a resolution of  $> 10^6$ .

The FIR/submm is extremely important for the investigation of both the galactic and extragalactic warm ( $T \sim 100$  K), interstellar medium. This material is heated by shock waves or UV radiation, phenomena that are often associated with star formation or other high energy events, e.g. supernovae or active galactic nuclei. This excited material then re-emits either as dust continuum radiation or gas line emission. CASIMIR will be able to utilize recent advances in the sensitivity of superconducting mixers to study the fundamental rotational transitions of many astronomically significant molecules, which cannot be observed with ground based telescopes, see Figure 1.

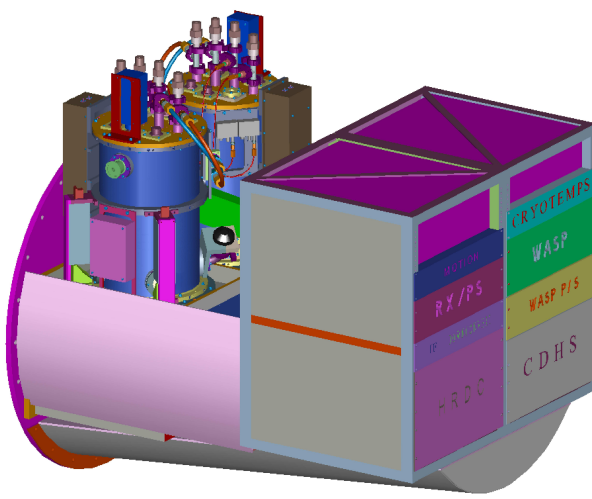


Fig. 2. The CASIMIR instrument. The instrument is mounted to the telescope via the round flange at extreme left of the figure. This flange forms the pressure interface between the telescope cavity and the aircraft's cabin. The portion of the instrument shown is located in the cabin, with the observers. The telescope beam enters the instrument through the center of this round flange, about 150 mm below the bases of the cryostats. The instrument structure is constructed almost exclusively of aluminum. It is approximately 1.5 m long by 1 m square. It weighs approximately 550 kg, including 150 kg of electronics mounted in the racks, at the right of the figure. Approximately 150 kg more of ancillary electronics are located elsewhere in the aircraft cabin.

## II. INSTRUMENT CONFIGURATION AND STRUCTURE

The general layout of the CASIMIR instrument is shown in Figure 2. Two cryostats are mounted side by side on top of a box, which contains the relay optics, see Section II-A.

Two 19-inch racks are mounted directly behind this box. All the critical electronics components are mounted in these racks, eg. the LO drive electronics and the microwave spectrometers. This ensures very short cable runs to the cryostat and prevents any differential rotation. All electronic systems for the instrument are packaged as 19-inch bins, which will allow easy replacement of any unit and reconfiguration of the electronics.

### A. Optics Box

Figure 3 shows a 3D model of the Optics Box, which is the mount for the cryostats and contains all the optics common to all frequency bands. The central feature is a plane mirror, which can be commanded to rotate through  $\pm 180^\circ$  in the plane of the telescope and up to  $\pm 5^\circ$  in tilt. This rotating mirror directs the telescope beam to one of the four elliptical mirrors mounted on the two cryostats, selecting the frequency band.

The calibration system consists of a chopper wheel at ambient temperature plus hot and ambient temperature loads. Moving the rotating mirror by  $\sim 180^\circ$ , allows any of the frequency bands to be first illuminated with the sky signal and then the signal from a known temperature calibration load.

CASIMIR will use the fully reflective tertiary mirror on SOFIA's telescope. As a result, none of the observatory's guiding cameras will be able to image the telescope's focal

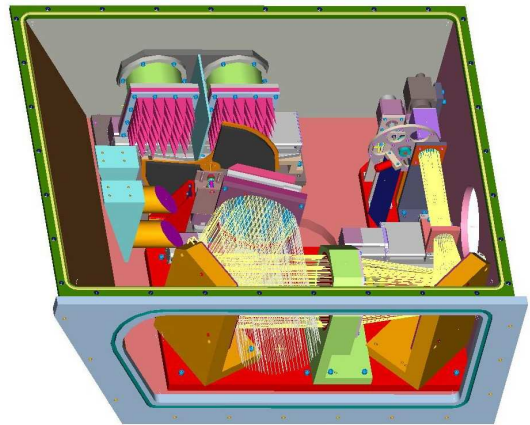


Fig. 3. The Optics Box. The cryostats are bolted directly to the lid of this box, which has been removed for this image. The elliptical mirrors mounted on the base of the cryostats protrude through an aperture in the lid and are located in the plane of the telescope beam. The two elliptical mirrors for one of the cryostats are shown in the left part of the image. The telescope beam enters from the front of the figure. In this image, the rotating mirror, at the center of the figure, directs the telescope beam to the optical boresight, at the far right rear corner. The calibration chopper wheel and the two loads are shown in the rear of the figure. The box forms part of the pressure interface between the aircraft cabin and the exterior, i.e. the box interior is exposed directly to the telescope cavity, so that at altitude, the pressure inside is  $\sim 200$  Torr. The wall thickness varies between 0.5 and 0.75 in.

plane. Therefore, we have included an optical boresight camera, inside the Optics Box, for alignment and beamfinding. The boresight can also be used as a pupil imager by moving a biconcave lens into the optical path. The camera has a  $6' \times 6'$  field of view and uses a 1024x1024 pixel, optical wavelength CCD. The rotating mirror also selects this camera.

Stepper motors are used to move all the optical components. All of these motors are mounted inside the Optics Box and are controlled remotely via software. There are only electronic feedthroughs mounted in the sides of the box, without any mechanical motions through the pressure boundary. Physical access to the Optics Box will not be required at any time during the flight.

### B. Cryostats

The cryostats are of conventional design with LN<sub>2</sub> and LHe reservoirs, see Figure 4. For frequencies below 1 THz, the mixers will operate at  $\sim 4$  K. At higher frequencies, we will pump on the LHe reservoir to operate the receivers at  $\sim 2.5$  K.

There will be two cryostats per flight and up to two frequency bands in each cryostat, so there will be up to four bands available per flight. Observations can be made with only one band at a time. Any one of the four bands can be selected at anytime during the flight. This selection is made by software alone, and does not require caging of the telescope, any mechanical adjustment or physical access to the instrument.

As shown in Figures 4 and 5, all the components specific to an individual frequency band are integrated directly onto the cryostat, eg. the LOs, IF systems and relay optics. All systems mounted elsewhere on the instrument are used for all of the bands. Therefore, the selection of the four bands which

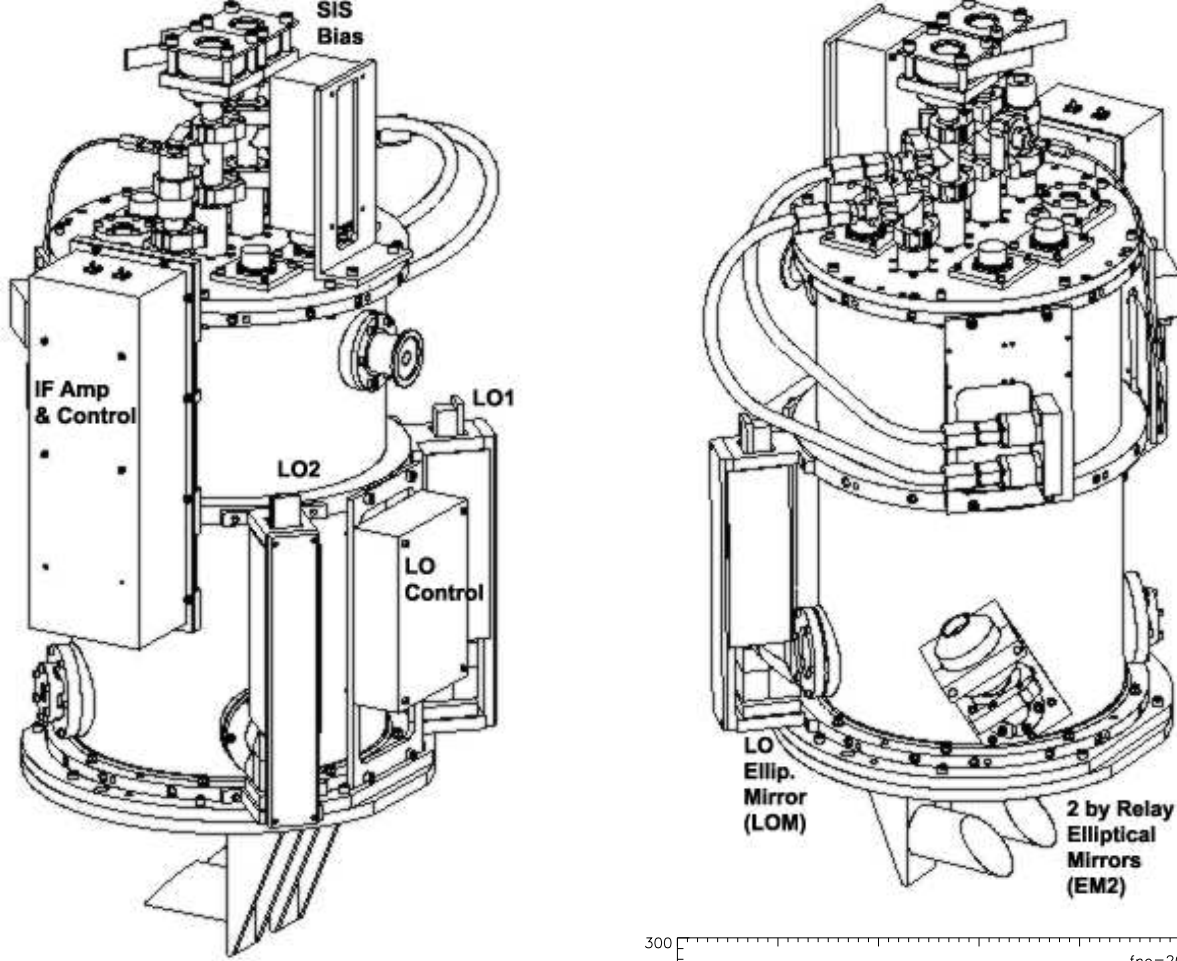


Fig. 4. The CASIMIR Cryostat. The cryostat contains 5 liters each of LN<sub>2</sub> and LHe and has a 250 mm diameter cold-work-surface. This is the maximum, practical diameter for cryostats that can be used in the side-by-side configuration for SOFIA. It is 600 mm high and weighs ~40 kg. The LOs, IF system, receiver and LO bias electronics are mounted directly to the side of the cryostat. The electronics for the cryogenic amplifier bias and mixer electromagnet current are also mounted on the cryostat but are not shown in this view. The two elliptical mirrors of the relay optics, mounted on the base of the cryostat, can be seen at the extreme bottom of the image.

are to be used on a given flight is determined by the choice of cryostats. Swapping of cryostats could easily be carried out between flights. Also, any upgrades and improvements to the bands could be accomplished independently of the rest of the instrument. This will allow continuous upgrades to the frequency bands, throughout the life of the instrument.

### C. Optics

Figure 5 shows a schematic of the relay optics, which uses two off-axis, elliptical mirrors to match the incoming telescope beam to the output beam of the mixer. Including the three telescope mirrors, there are five mirrors at ambient temperature and one cryogenically cooled mirror, EM1, in the optical train.

The window in the base of the cryostat is the only pressure boundary in the optical path from the telescope. Therefore, this window and a lens in the mixer assembly are the only

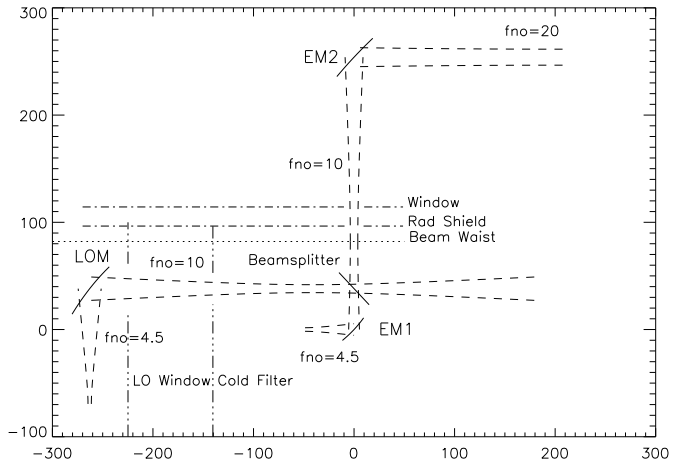


Fig. 5. CASIMIR Relay and LO Injection Optics. The top image shows the location of the elliptical mirrors mounted on the cryostat. The bottom part of the image shows a schematic of the optics. In the lower image, the up down orientation is reversed and the units on the scale are mm, with the origin at the center of EM1, the elliptical mirror mounted on the cryostat cold-work surface. EM2 is the elliptical mirror mounted below the base of the cryostat, visible in the upper image. EM2 is in the plane of the telescope beam, it converts the incoming, diverging  $f/\# \sim 20$  telescope beam into an intermediate  $f/\# \sim 10$  beam and reflects it through  $90^\circ$ , through a window in the base of the cryostat. LOM is the LO elliptical mirror, which matches the LO output beam to the incoming intermediate beam. EM1 converts the intermediate beam to a converging  $\sim f/\# 4.5$  beam, which matches the output beam of the mixer.

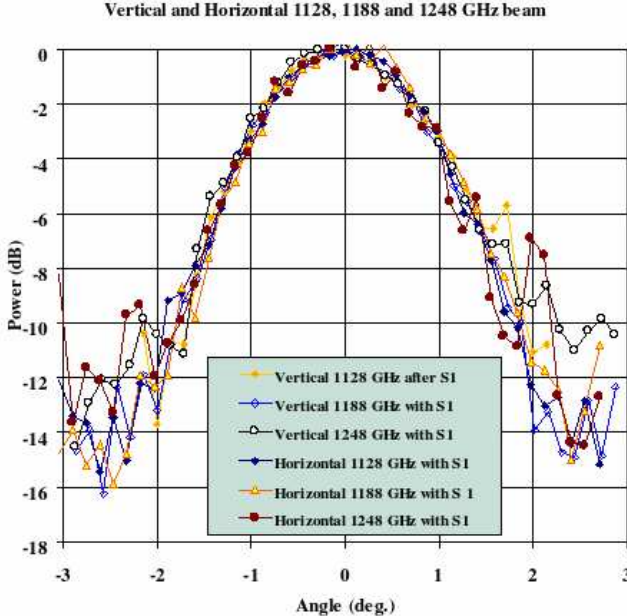


Fig. 6. Measurements of the output beam profile of the 1.2 THz mixer. The image consists of 6 curves overlaid on each other. These curves are vertical and horizontal scans through the output beam after the second elliptical mirror, EM2 in Figure 5. These scans were taken at three separate frequencies across the 1.2 THz band.

transmissive elements in the entire optical train from the telescope to the receiver.

The optical designs for all bands have an edge taper of 10 dB. Aperture and main beam efficiencies are calculated to be 0.71 and 0.77, respectively. The largest beam size is 0.8 arcmin, at 550 GHz.

Figure 6 shows measurements of the mixer beam after the second elliptical mirror. There is little evidence of distortion or chromatic aberration. The measured  $f/\#$  is  $>18$ , as opposed to the design point of 20.7. This is the first iteration of our mixer optics. This faster beam would reduce our aperture efficiency on the telescope, but is suitable for continued lab testing. Further iterations should remedy this. These measurements are discussed in detail elsewhere in these proceedings[5].

#### D. Mixers

The mixers for all 5 bands will be Nb/AlN/NbTiN, quasi-optically coupled, superconducting-insulating-superconducting (SIS), twin-slot mixers. The development of these mixers is discussed elsewhere in these proceedings[6].

### III. MICROWAVE BACK END SPECTROMETER

We have acquired a field-programmable gate array (FPGA) based, fast Fourier transform (FFT), microwave backend spectrometer from Omnisys Instruments[7], see Figure 7. The spectrometer consists of a variable number of modules covering an IF band of 4 GHz each.

Each of these modules consists of three cards;

- two FPGA digitizer and correlator cards, each with a 2 GHz bandwidth,

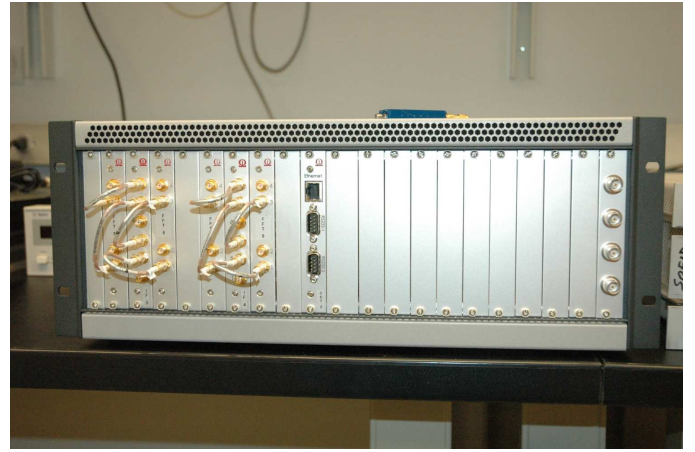


Fig. 7. Omnisys FPGA based FFT microwave spectrometer. In this image, the rack bin is only half populated, with two 4 GHz IF modules, i.e. two sets of three cards, giving a total IF coverage of 8 GHz. The center card in each set of three, is the IF processor. The cards have a single height Eurocard format and are mounted in a 4U, 19" rack bin. As displayed, the system weighs 12.5 kg and dissipates less than 200 W. During initial flights on SOFIA, only a single module would be used. If both halves of the rack were populated, a single unit could cover an IF passband of 16 GHz. Therefore, depending on the number of installed modules, this single rack bin can be readily configured to cover an IF range of 4, 8, 12 or 16 GHz.

- and an integrated IF downconverter and processor card, which uses IQ mixers to distribute the 4-8 GHz IF passband to the two digitizer cards.

There is some overlap in the outputs from the digitizer cards, and the total useful IF bandwidth of the spectrometer has been measured to be 3.8 GHz. Efforts are underway to reduce this overlap and to recover the full 4 GHz IF coverage.

The frequency resolution has been measured to be 268 KHz, i.e. over 14,000 usable channels. At 1 THz, this corresponds to a resolution greater than  $3 \times 10^6$ , or 800 m/s.

#### A. Tests at CSO

In October, 2009, the spectrometer was used to carry out observations at the Caltech Submillimeter Observatory (CSO), using the 230 GHz wide band receiver, aka Frank's Receiver[8]. During these observations, we used two of the digitizer correlator cards and an external IF processor which yielded a IF bandpass of 4-8 GHz. Figures 8 and 9 show examples of the spectra obtained during this run.

We expect to take a spectrometer with 8 GHz of IF coverage to the CSO in the middle of this year.

### IV. LOCAL OSCILLATORS AND FREQUENCY BANDS

The Local Oscillators (LOs) for all bands are tunerless and use solid state devices exclusively. LOs for the lower frequency bands, below 900 GHz, have been acquired from Virginia Diodes Inc. (VDI)[9]. LOs for the higher frequency bands were developed at JPL for CASIMIR. The development of the LOs at JPL is discussed elsewhere in these proceedings[10].

As shown in Figure 4, up to two LOs can be mounted directly to the side of the cryostat. The LO output is via a feedhorn. The output divergent beam is reflected through 90° and converted into a  $\sim f/\#10$  converging beam, by an off-axis, elliptical mirror, mounted directly below the feedhorn,

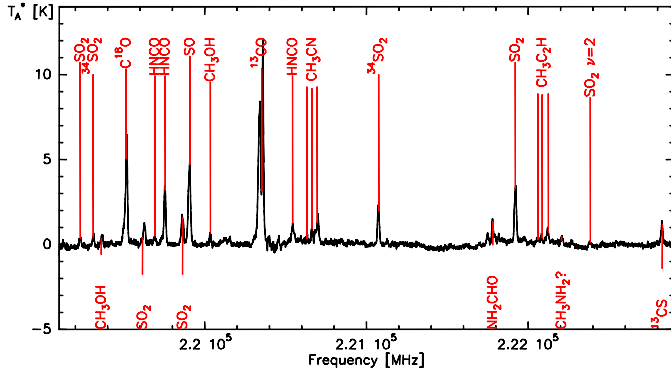


Fig. 8. Spectrum of the Galactic Center, centered on 221 GHz. This spectrum displays the full usable 3.8 GHz IF bandwidth of the spectrometer. This data was obtained with position switching under marginal conditions,  $\tau = 0.18$ .

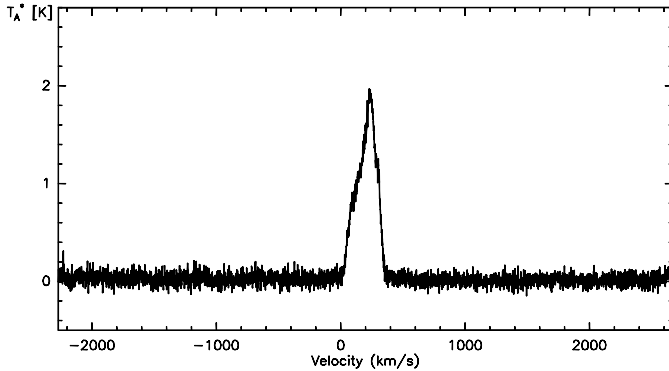


Fig. 9. Spectrum of M82 observed in the  $^{12}\text{CO}$  2-1 line. The line width is approximately 400 km/s. Note the extremely flat continuum.

see Figure 5. The beam passes through a window in the cryostat wall to a mylar beamsplitter mounted directly below the receiver elliptical mirror, EM1. The beamsplitter directs a portion of the LO signal power towards the cryostat cold work surface, combining it with the incoming, astronomical signal.

#### A. LO Drive System

1) *LO Drive Signals and Conditioning.*: All bands are driven from a single, commercial, microwave synthesizer, an Anritsu MG3694[11], at a frequency in the range 26-40 GHz. Immediately after the synthesizer, the LO drive signals are conditioned via the LO Drive Unit (LDU), containing a single YIG filter and power amplifier, see Figure 10.

Figure 11 compares the IF output from a mixer pumped by the same LO, with and without the LDU. The artifacts from the microwave frequency synthesizer are completely removed by the YIG filter.

Figure 12 compares the mixer noise temperature of a mixer pumped by a synthesized, solid state, tunerless LO and a Gunn Diode based LO. With the YIG filtering on the synthesizer output, we obtain equivalent performance for these two types of LOs.

The output from the LDU will be used to drive all the four LO chains, on any given flight. Only one chain will be driven at any given time. Any one of four bands can be selected completely via software at anytime during the flight, without any mechanical adjustment.

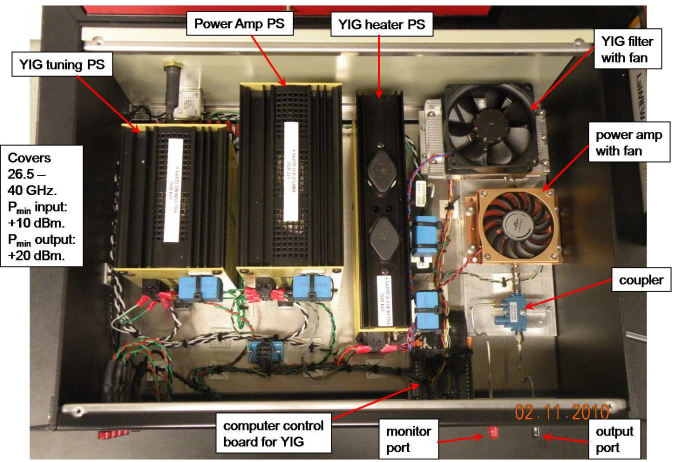


Fig. 10. The LO Drive Unit (LDU). This unit contains a single YIG Filter and power amp. It is located immediately adjacent to the microwave frequency synthesizer. The LO drive signals for all four frequency bands, on a given flight, will be routed through this unit. This is a lab prototype, completely filling a 4U 19" rack bin. Significant effort will be required to produce a lighter, more compact flight unit.

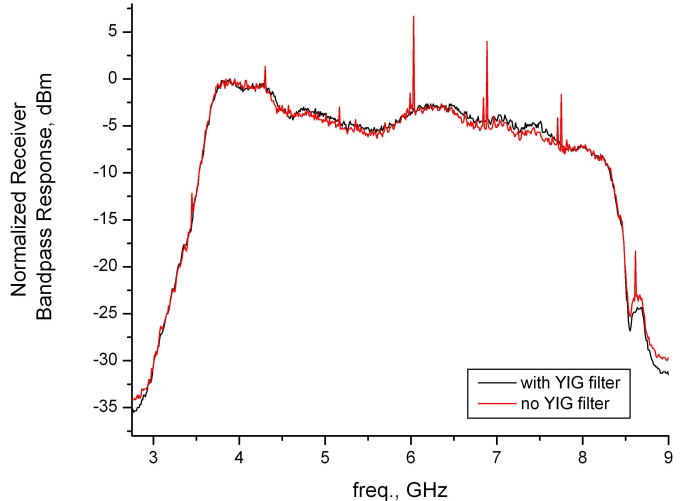


Fig. 11. Comparison of the IF output from an SIS mixer driven by a solid state 500 GHz LO, with and without the LDU. The same LO drive signal, from the microwave frequency synthesizer, was used for both curves. The lighter line does not use the YIG filter and the dark line does.

2) *The First Stage of the LO Chains*: On the aircraft, the first stage will be the same for each LO multiplier chain. One of these first stages will be dedicated to each chain. This first stage will have an output of 78-120 GHz and consists of;

- 1) a VDI tripler,
- 2) a W10 isolator,
- 3) a W10 Spacek amplifier,
- 4) a W10 isolator.

At present, each of our existing LO chains uses this first stage, except the 750 GHz LO, see Section IV-C. Figure 13 shows an example of a full LO multiplier chain.

### C. 750 GHz

We have acquired a 750 GHz LO from VDI. Figure 14 shows the output power spectrum and the LO itself. The 750 GHz LO is intended to cover the 690 to 840 GHz frequency range. The coverage of this large fractional bandwidth,  $\sim 20\%$ , requires two parallel chains, for the low and high frequency parts of the band. The input from these chains is fed into a common, final multiplier, via a microwave switch. This arrangement provides good power levels across the band of interest, with up to  $\sim 80 \mu\text{W}$  at the most interesting line,  $\text{H}_2\text{O}^{18}$  at 745 GHz.

### D. 1 THz

Figure 15 shows the output power and multiplier chains for the LOs covering the 1 THz band. These LOs were manufactured at JPL for CASIMIR.

The frequency range for this band covers 800 to 1050 GHz. Such a large fractional bandwidth, 27%, cannot be covered by a single multiplier chain. So the band must be split into two sub-bands, nominally 900 GHz and 1 THz, with a separate multiplier chain for each of them.

The lines of most astronomical interest, e.g.  $\text{CH}_2$  (946 GHz),  $\text{NH}$  (975 GHz),  $\text{H}_3\text{O}^+$  (985 GHz),  $\text{H}_2\text{O}^{18}$  (995 GHz) and  $\text{CO}$  (1037 GHz) are all located in the upper sub-band. The 1 THz LO has good coverage,  $> 50 \mu\text{W}$  for most of these lines.

Many of the frequencies in the lower sub-band are observable from the ground, so there may be relatively little demand for this sub-band on SOFIA. We intend to fly the 1 THz sub-band in the default configuration for CASIMIR. If there is a request to observe in the 900 GHz sub-band, we would use the same mixer, but replace the 1 THz LO with the 900 GHz chain. At this stage, we do not intend to have both of these sub-bands available on any one flight.

### E. 1.2 THz

Figure 16 shows the output power for the multiplier chain for the 1.2 THz LO. This chain was developed at JPL. The frequency range for this band is 1.1-1.2 THz, and it is covered with power levels from 30-90  $\mu\text{W}$ . The most significant frequencies, the four  $\text{H}_2\text{O}^{18}$  lines, are well covered with LO power levels  $> 60 \mu\text{W}$  for all of them. The next most interesting line, HF at 1.23 THz, may be difficult to observe due to the relatively low LO power,  $< 30 \mu\text{W}$ , and the high atmospheric absorption at that frequency.

### F. 1.4 THz

Figure 17 shows the output power for the multiplier chain for the 1.4 THz LO. This chain is still under development at JPL. At present, the power output over the region of interest is in the range 40 – 70  $\mu\text{W}$ . However, it is possible that this may improve. The most important frequency in this band is the  $\text{H}_2\text{D}^+$  line at 1.37 THz, which is well covered with LO power levels  $> 50 \mu\text{W}$ . The next most interesting line,  $\text{N}^+$  at 1.46 THz, lies at the extreme high frequency end of the LO's output and probably cannot be observed.

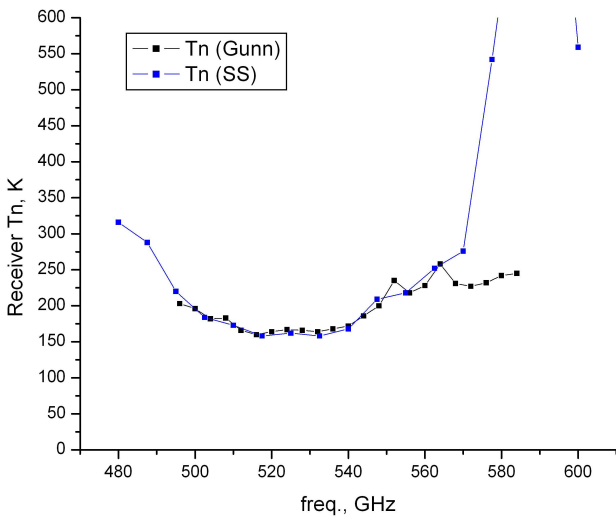


Fig. 12. Comparison of the receiver noise temperature from a SIS mixer pumped by a synthesized, solid-state LO and a Gunn diode based LO. The increase in noise at the high frequency end of the bandpass, for the solid state LO, is not due to the LO drive signal. It is due to bandpass limitations on the high frequency multiplier, see Section IV-B.

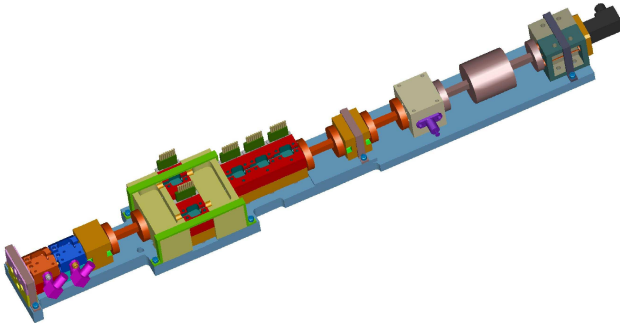


Fig. 13. The complete LO Chain for the 1.2 THz band. The first stage of the multiplier chain occupies the right half of the diagram. The high frequency part of the chain, i.e. frequency multiplication above 120 GHz, is shown in the left half of the figure and is also shown in Figure 16. This chain is expected to be the longest used on the instrument. It will be approximately twice as long as the LO assemblies shown in Figure 4, and will extend slightly beyond the top of the cryostat itself.

### B. 500 GHz

The 500 GHz channel is intended to cover the 500 to 640 GHz passband. The most important line in this region is the  $\text{H}_2\text{O}^{18}$  line at 547 GHz. The other interesting lines are  $\text{CH}$  (532 and 536 GHz),  $\text{NH}_3$  (572 GHz) and  $\text{CO}$  (576 GHz).

At present, we are using a single VDI quintupler as the high frequency multiplication stage. However, its output is limited to  $\sim 570$  GHz. We are now investigating using a x2x3 combination of VDI multipliers, in order to extend the coverage up to 640 GHz.

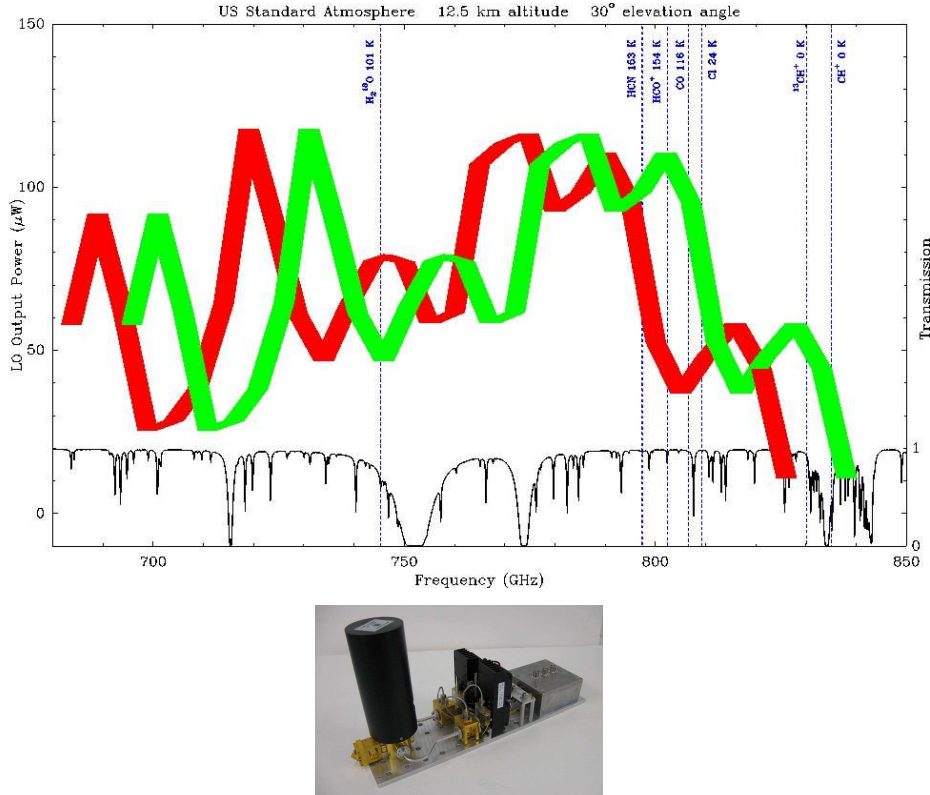


Fig. 14. Frequency coverage of the 750 GHz band and the existing complete 750 GHz LO. The plot shows the LO output power superimposed on the atmospheric absorption at SOFIA's operating altitude. The significant astronomical, spectral lines are also shown. The light and dark LO output power curves, respectively, represent the upper and lower side bands, for a given frequency tuning. The large black object at the left of the photograph of the LO, is the microwave switch for selecting the high or low multiplying chain. Some effort will be required to reconfigure this LO for flight.

## V. CONCLUSIONS

CASIMIR is a FIR/Submm, heterodyne spectrometer for SOFIA. It is well suited for the studies of the warm ( $T \sim 100K$ ) interstellar medium, particularly water, measuring many significant lines unobservable from the ground. Initially, the instrument will cover 5 bands in the frequency range from 0.5 to 1.4 THz.

A very high resolution backend spectrometer has been successfully tested. It provides continuous coverage of 3.8 GHz of IF bandwidth with a resolution  $> 10^6$ , across the whole frequency range of the instrument.

LO chains suitable for flight are available for the three frequency bands of 1 THz or higher and candidate chains are available for the two lower frequency bands. With conditioning of the LO drive signals, the synthesized, solid state LOs will provide performance equivalent to those based on Gunn diodes.

The instrument design is extremely modular. CASIMIR will be able to continuously incorporate new hardware, to accommodate future improvements in mixer, LO and backend spectrometer technology, for some time to come.

## VI. ACKNOWLEDGMENTS

Various subsystems of the CASIMIR instrument have been, or continue to be developed, by a number of people at several institutions: J. Stern and H. G. LeDuc, Micro Devices Lab, JPL (mixer fabrication), M. R. Haas, NASA Ames (optics), the Kosma I/O Team, U. of Koln and S. W. Colgan, NASA

Ames (software), and S. Lin, Caltech/JPL (mechanical design). The development of CASIMIR is supported by NASA/USRA SOFIA Instrument Development Fund.

## REFERENCES

- [1] M. L. Edgar, A. Karpov, S. Lin, D. Miller, S. J. E. Radford & J. Zmuidzinas, "CASIMIR, The Caltech airborne submillimeter interstellar medium investigations receiver", *SPIE*, **7020**, 702012 (2008).
- [2] E. E. Becklin, A. A. G. M. Tielens, R. D. Gehrz & H. H. S. Calis, "Stratospheric Observatory for Infrared Astronomy", *SPIE*, **6678**, 667880A, 2007.
- [3] S. C. Casey, "The SOFIA program: astronomers return to the stratosphere", *SPIE*, **6267**, 2006.
- [4] E. E. Becklin, A. G. G. M. Tielens & H. H. S. Callis, "Stratospheric Observatory for Infrared Astronomy (SOFIA)", *Mod. Phys. Lett. A*, **21**, 2551-2560, 2006.
- [5] A. Karpov, D. Miller, M. Emprechtlinger, M. Edgar, F. Rice, A. Harris, J. A. Stern, H. G. LeDuc & J. Zmuidzinas, "Characterization of 1.2 THz SIS receiver for CASIMIR", *these proceedings*.
- [6] A. Karpov, D. Miller, J. A. Stern, F. Rice, H. G. LeDuc & J. Zmuidzinas, "1.4 THz SIS mixer using Nb and Al tuning circuit", *these proceedings*.
- [7] Omnisys Instruments AB, Gruvgatan 8, SE-421 30 Vastra Frolunda, SWEDEN, [www.omnisys.se](http://www.omnisys.se)
- [8] F. Rice, M. Sumner, J. Zmuidzinas, R. Hu, H. LeDuc, A. Harris & D. Miller, "SIS mixer design for a broadband millimeter spectrometer suitable for rapid line surveys and redshift determinations", *SPIE*, **4855**, 301-311, 2002.
- [9] Virginia Diodes Inc., 979 Second St. S.E., Suite 309, Charlottesville, VA 22902-6172, USA, [virginiadiodes.com](http://virginiadiodes.com)
- [10] R. Lin, B. Thomas, J. Ward, A. Maestrini, E. Schlecht, J. Gill, C. Lee, S. Sin, F. Maiwald & I. Mehdi, "Development of Local Oscillator Sources for CASIMIR", *these proceedings*.
- [11] Anritsu Company, 490 Jarvis Drive Morgan Hill, CA 95037-2809, USA, [www.us.anritsu.com](http://www.us.anritsu.com)

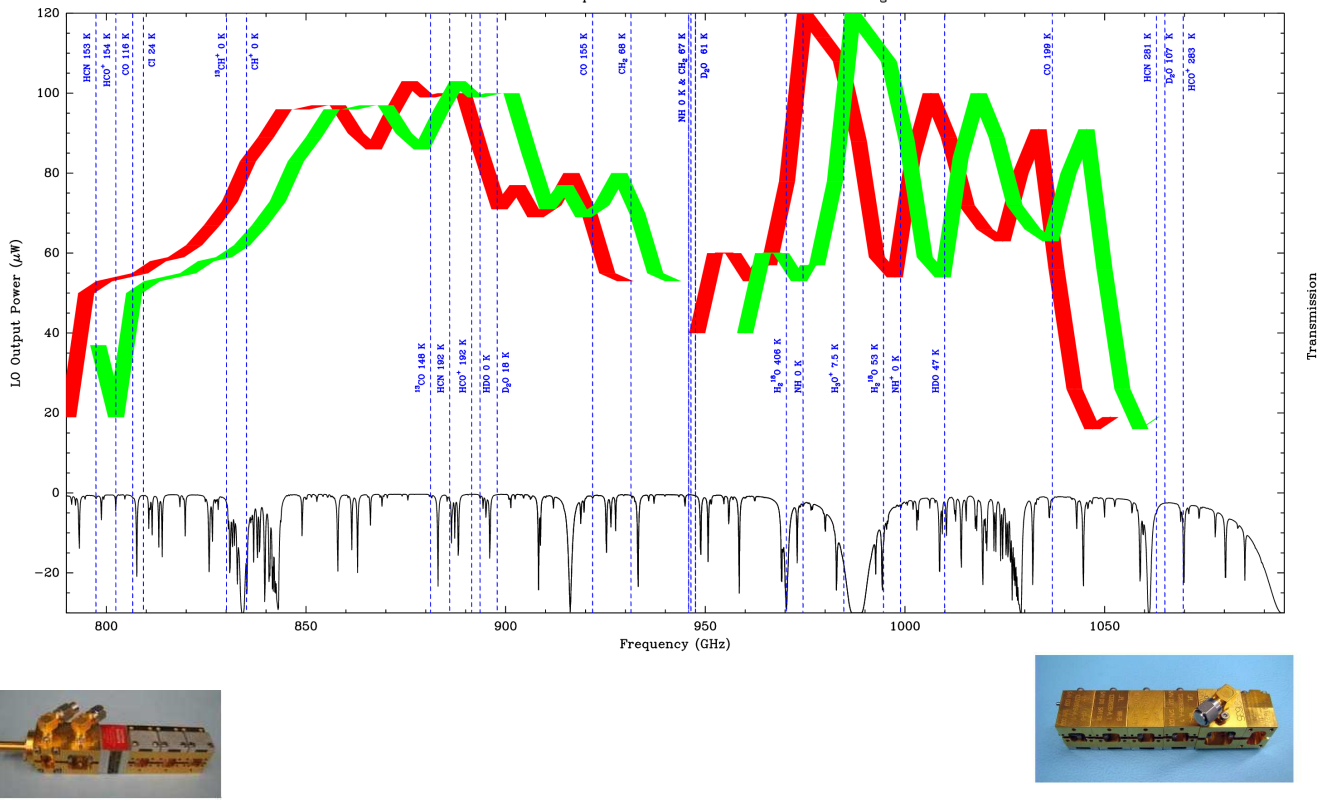


Fig. 15. Frequency coverage of the 1 THz band and the 900 and 1000 GHz LOs. The format of the diagram is similar to that in Figure 14. The high frequency portions of the multiplier chains are shown below the main figure, the 900 GHz to the left and the 1 THz on the right.

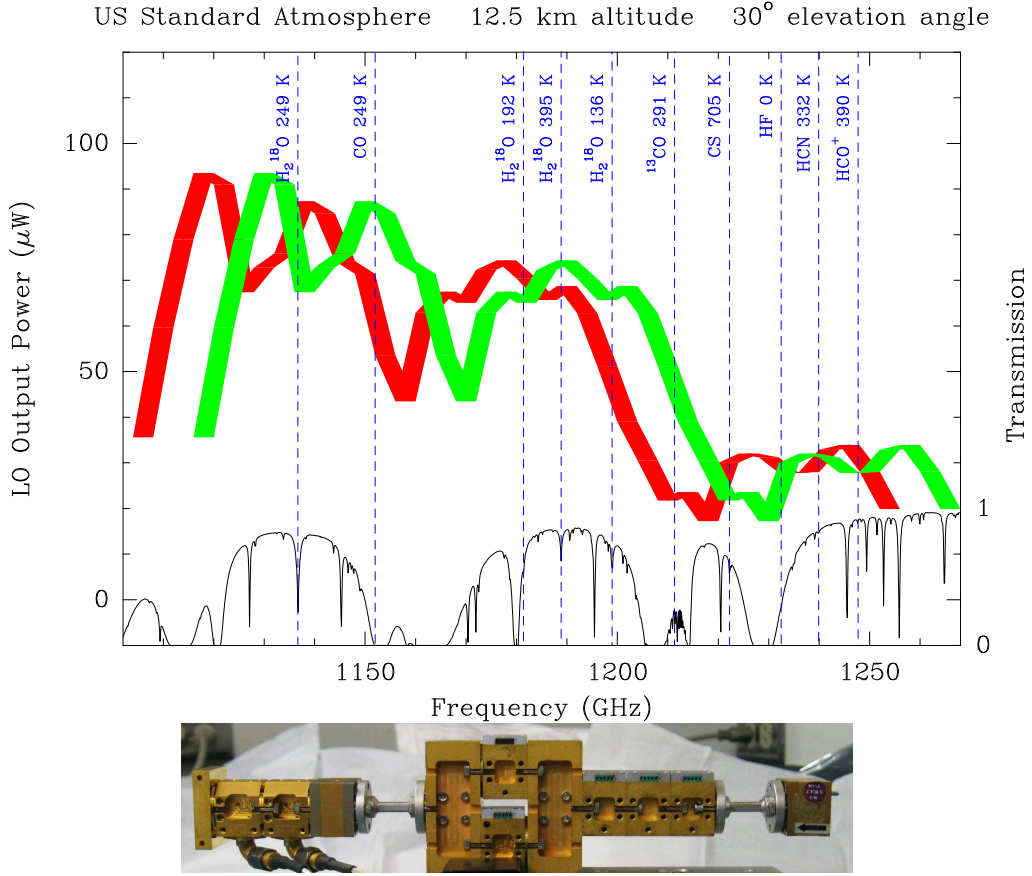


Fig. 16. Frequency coverage of the 1.2 THz band and the high frequency portion of the multiplier chain for the 1.2 THz LO. The format of the diagram is similar to that in Figure 14.

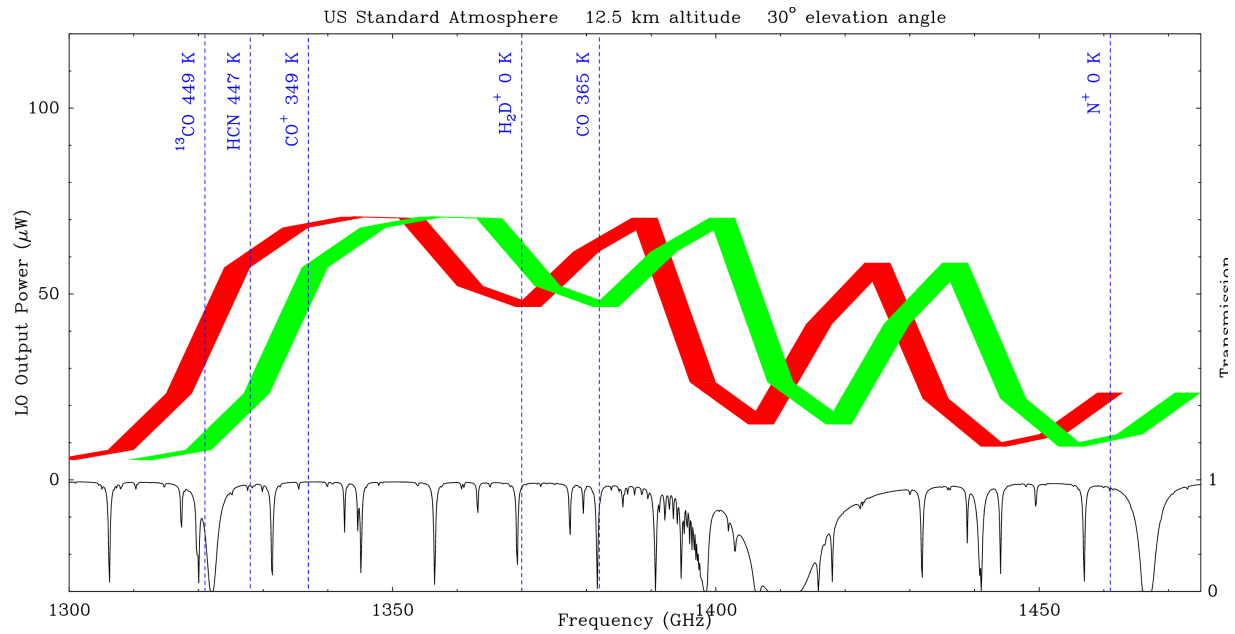


Fig. 17. Frequency coverage of the 1.4 THz LO. The format of the diagram is similar to that in Figure 14.